ANALYTICAL STUDY OF YTTRIA BASED MEMRISTIVE SYSTEM

M.Tech. Thesis

By

PRATYUSH MISHRA

DISCIPLINE OF ELECTRICAL ENGINEERING

INDIAN INSTITUTE OF TECHNOLOGY INDORE

JUNE 2020

ANALYTICAL STUDY OF YTTRIA BASED MEMRISTIVE SYSTEM

A THESIS

Submitted in partial fulfillment of the requirements for the award of the degree

of

Master of Technology

by

PRATYUSH MISHRA

DISCIPLINE OF ELECTRICAL ENGINEERING

INDIAN INSTITUTE OF TECHNOLOGY INDORE

JUNE 2020

4323

INDIAN INSTITUTE OF TECHNOLOGY INDORE

CANDIDATE'S DECLARATION

I hereby certify that the work which is being presented in the thesis entitled **ANALYTICAL STUDY OF YTTRIA BASED MEMRISTIVE SYSTEM in** thepartial fulfillment of the requirements for the award of the degree of **MASTER OF TECHNOLOGY** and submitted in the **DISCIPLINE OF ELECTRICAL ENGINEERING,Indian Institute of Technology Indore**, is an authentic record of my own work carried out during the time period from July 2019 to June 2020 under the supervision of Dr. Shaibal Mukherjee, Associate Professor, Indian Institute of Technology Indore

The matter presented in this thesis has not been submitted by me for the award of any other degree of this or any other institute.

Mishra
16/06/2020
PRATYUSH MISHRA

This is to certify that the above statement made by the candidate is correct to the best of my/our knowledge.

S. Mukherjee
Thesis Supervisor

Dr. SHAIBAL MUKHERJEE

PRATYUSH MISHRA has successfully given his M.Tech. Oral Examination held on **June 22, 2020**.

S. Mukherjee 22/6/2020
Signature(s) of Supervisor (s) of M.Tech. Thesis
Date:

Convener, DPGC
Date: 22/6/2020

22/6/2020 (Mukesh Kumar)
Signature of PSPC Member #1
Date:

(Dr. A. K. Das)
Signature of PSPC Member #2
Date: 22/6/2020

ACKNOWLEDGEMENTS

I would like to express my sincere gratitude to my thesis supervisor **Dr. Shaibal Mukherjee**, Associate Professor for his constant support, encouragement and guidance during my Master's study and thesis work. Furthermore, I would like to express my deep gratitude to my PSPC members **Dr. Mukesh Kumar** and **Dr. Apurba K. Das** for their valuable suggestions and feedback.

I would like to thanks **Dr. Santosh Kumar Vishwakarma**, as he helped us in the domain of course work as well introduced us to a whole new level of perspective of electrical discipline.

I would also like to thanks **Mr. Sanjay Kumar** for giving me valuable comments regarding the problem related to modeling and coding.

I would at so like to thank H.N.R.G research group for supporting a friendly and environment in the laboratory.

My gratitude to **Mr. Sagar Rana, Mr. Prashant Puri** and all my M.Tech batch mates for the wonderful experience I had with them in these course of time as they all helped me in my project in ways which are not quantifiable yet important.

IIT Indore played a vital role in providing me with the facilities, teaching assistantship, hostel accommodation and lab computer and library resource that added to my knowledge and my project.

All this was made possible by incredible support and blessings of my parents who blessed me all the time, it would not have been possible without their love and support.

ABSTRACT

Before 1971, all the electronic circuits were based on three basic circuit elements. Until a professor from UC Berkeley reasoned that another basic circuit element exists, which he called memristor; characterized by the relationship between the charge and the flux-linkage. A memristor is essentially a resistor with memory. The resistance of a memristor (Memristance) depends on the amount of current that is passing through the device. In 2008, a research group at HP Labs succeeded to build an actual physical memristor. HP's memristor was a nanometer-scale titanium dioxide thin-film, composed of two doped and undoped regions, sandwiched between two platinum contacts. After this breakthrough, a considerable amount of research started with the aim of better realization of the device and discovering more possible applications of the memristor.

Since the advent of the memristor as an actual basic element, a significant thrust of the research has been oriented to develop neuromorphic computing system based on memristor. Neuromorphic computing and learning behavior are among the most directly available applications of memristor due to its memory property.

Here, an analytical model for Y_2O_3-based memristive system for synaptic learning behavior has been reported. In this analytical model, a new logarithmic window function is used along with modified I-V relationship to show the asymmetric behavior in both positive and negative voltage biases and thus provides a good accuracy with the published experimental report.

TABLE OF CONTENTS

LIST OF FIGURES

LIST OF TABLES

LIST OF ABBERIVIATION

Abbreviations	Description
HRS	High resistance state
LRS	Low resistance state
LCS	Low conducting state
HCS	High conducting state
RRAM	Resistive random access memory

Chapter 1

Introduction

1.1 Overview

In the circuit logic, reference is made to the presence of three basic circuit elements describing the interaction between the basic circuit parameters such as voltage(v), current(i), charge(q), and magnetic flux(ϕ). These are resistors, capacitor, and inductor. However, the circuit element that determines the relationship between charge and magnetic flux is not specified. The fourth basic circuit component representing this relationship was first introduced by Leon Chua mathematically in 1971 with the name memristor [1]. In 2008, a team of researchers from HP laboratories announced that they were working to produce a physical model of a memristor [2]. Figure (1.1) shows the relationship between the basic circuit elements and circuit parameters.

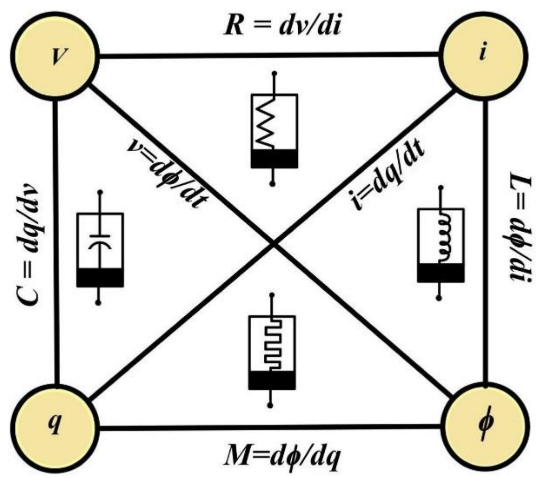

Figure 1.1. Linkage between four fundamental elements and basic circuit parameter such as voltage(v), current(i), charge(q), and magnetic flux(ϕ).

The relationship between voltage, current, charge, and flux for the memristor is given by:

$$v(t) = M\big(q(t)\big)i(t) \tag{1.1}$$

$$M(q) = \frac{d\phi(q)}{dq} \tag{1.2}$$

$$i(t) = W\big(\phi(t)\big)v(t) \tag{1.3}$$

$$W(\phi) = \frac{dq(\phi)}{d\phi} \tag{1.4}$$

where $W(\phi)$ has the unit of conductance and $M(q)$ has the unit of resistance.

Memristor shows different properties compared from other fundamental circuit elements that are pinched hysteresis loop, passivity, and non-volatile memory effect.

When Equation (1.1) and (1.22) are analyzed, Equation (1.5) and (1.6) can be written as follows:

$$v(t) = M\left(\int_{-\infty}^{t} i(t)dt\right) i(t) \quad (1.5)$$

$$i(t) = M\left(\int_{-\infty}^{t} v(t)dt\right) v(t) \quad (1.6)$$

The current passing through the memristor tells about the memristance value. That means, when the current flow through memristor is off, it retains the value of the memristance, and when the current flow through the memristor is passed again, memristance value will change from the last retained value, i.e. before the cutoff. That shows the non-volatile property of memristor and also tells about that, the memristor is not an energy storage element [3, 4].

Memristor is analogous to a resistor with memory [5]. The I-V curve of memristor shows the pinched hysteresis loop characteristic.

If a bipolar signal periodic in nature is applied to a memristor it shows a pinched hysteresis I-V characteristic that always crosses the origin. As the frequency of the applied signal increases the pinched hysteresis loop shows the singled valued function and behaves as a linear resistor. When the frequency reaches to infinity, the pinched hysteresis loop behaves as a single-valued function which has resemblance with resistor following ohms law [6, 7].

The memristor is a passive circuit element which can remember the state of resistance because of the voltage-current integral relationship. Because of these features, they are used soft computing, in resistive memories, neurocomputing, etc.

1.2 Modeling of memristor

1.2.1. HP memristor model

Memristor-based applications require an appropriate model for analysis and simulation of the system. Going through the literature, we can see that HP memristor model works on the principle of the drift of oxygen vacancies. The HP Lab memristor model composed of Pt/TiO_2/Pt structure, as shown in Figure (1.2). In HP labs model, a positively charged oxygen vacancies are present at one side of the TiO_2 oxide layer, which is sandwiched between the two noble metallic layers, i.e. platinum [2].

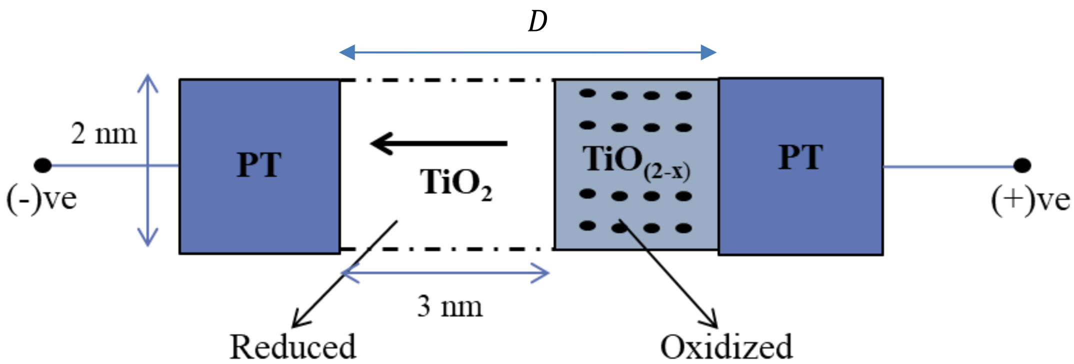

Figure.1.2: The structure of TiO_2-based memristor developed by HP Labs.

The doped part of oxide layer shows the low resistance behavior while the high resistance behavior is demonstrated by an undoped portion of the oxide layer. On an application of appropriate supply, the ionic drift between the doped portion and therefore the undoped portion leads to a change in the width of the doped region.

Here the width of the doped region is taken as a state variable. Also, when the width of the doped region approaches zero, the memristor goes to a high resistance state (HRS). When the width of the doped region approaches a boundary, the memristor goes to a low resistance state (LRS).

Since the dimensions of memristor are very small (~nm), a low excitation in the supply can cause a change in the doped region. Thus the resistance of the memristor varies between HRS and LRS [3].

1.2.2. Linear drift model

In the linear drift model, the relation between the current and the voltage of the memristor is given by the following equation:

$$v(t) = M(x)i(t) \tag{1.7}$$

$$v(t) = \left[\left(\frac{R_{ON}\, x(t)}{D}\right) + R_{OFF}\left(1 - \frac{x(t)}{D}\right)\right] i(t) \tag{1.8}$$

Here width of doped region $= x(t)$, memristor device thickness = D and R_{ON} and R_{OFF} (maximum and minimum resistance) are the values of the resistance for $x(t) = D$ and $x(t) = 0$ [2, 8, 9], From Equation (1.8), the value of memristance can be expressed by

$$M(q(t)) = \frac{v(t)}{i(t)} = \left[\left(\frac{R_{ON}\, x(t)}{D}\right) + R_{OFF}\left(1 - \frac{x(t)}{D}\right)\right] \tag{1.9}$$

Here $x(t)$ value represents the state of the change of memristor shown in Equation (1.8). The dx/dt in Equation (1.10) represents the rate of change of boundary between doped and undoped region [12, 13].

$$\frac{dx(t)}{dt} = \mu_v \frac{R_{ON}}{D}\, i(t) \tag{1.10}$$

Where μ_v = average drift mobility of the charges.

Figure (1.3) and (1.4) shows the change of the voltage and current of the memristor with time. The pinched hysteresis loop in the I-V plane shown in Figure (1.5) is one of the most important footprint of the memristor [1].

The I-V pinched hysteresis loops area decreases as we keep on increasing the frequency (F3>F2>F1). If the frequency increases toward infinity, the I-V characteristic shows the linear resistance characteristic.

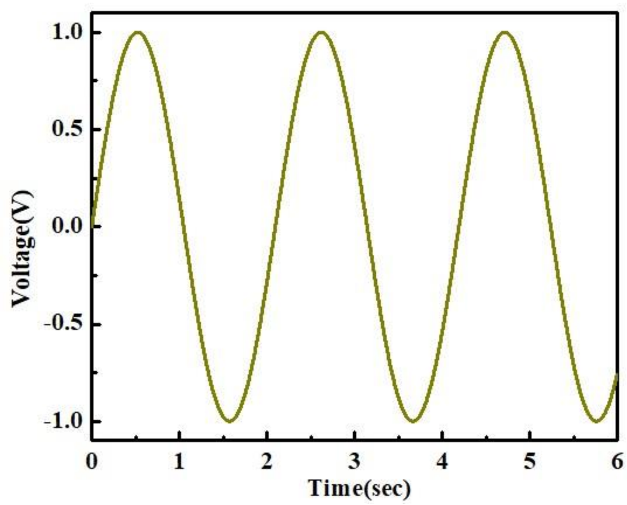

Figure 1.3. Change of voltage with respect to time.

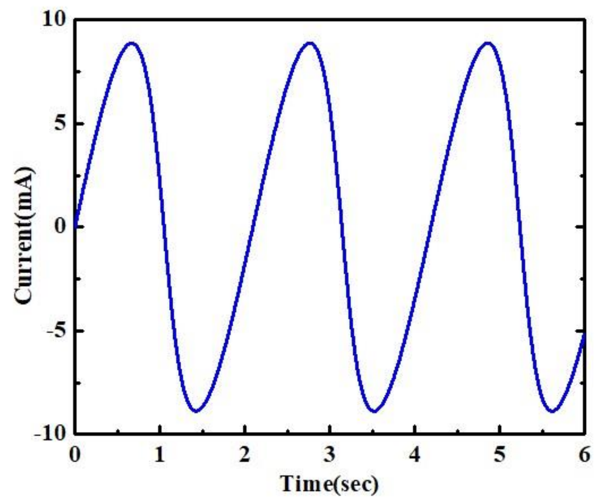

Figure 1.4. Change of current with respect to time.

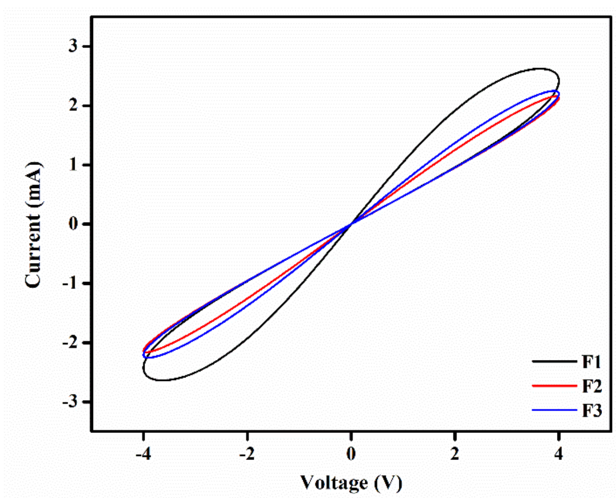

Figure 1.5. Current-voltage characteristics for varying frequency.

1.2.3. Nonlinear drift model and window functions

The charge flowing in the memristor is proportional to the state variable in the linear drift model, and the concept is used for doped and undoped interface and interface between electrodes. The doped region portion changes with the applied input signal. Also, in the linear drift model, the vacancies can drift over the complete length of a memristor. In the reported literature, the drift of vacancies is non-linear near the boundary interfaces region. That is due to the non-linear drift of vacancies caused by a large electric field even for a small excitation signal. Another problem in the linear drift model is non-zero boundary conditions, i.e. the state variable never reaches zero. Which indicates the absence of oxygen vacancies and due to the lack of undoped region, the doped region cannot take the complete length because of which memristor cannot work [13, 14, 15].

To overcome the boundary problems and to provide nonlinearity, a window function is introduced to the right of the equation (1.10).Which is given as

$$\frac{dx(t)}{dt} = \mu_v \frac{R_{ON}}{D} i(t) \times f(x(t)) \tag{1.11}$$

Function $f\big(x(t)\big)$ is zero at the memristor limits ($x = 0 \; and \; x = 1$) and has a maximum value at center of the memristor ($x = 0.5$) [11].

An effective window function should satisfy the subsequent conditions for modelling of nonlinearity [16]:

- The boundary situation should be taken into consideration at the bottom and top electrodes.
- The window function should provide non-linear drift across the whole active area of the memristor.
- The window function should provide linkage between the linear and non-linear drift models.
- The window function should lie in the interval of $fmax(x)$ i.e. $0 \leq fmax(x) \leq 1$.
- The window function should include some of the control parameters to line the model.

To provide the above criteria's many window function are proposed.

1.2.4. Joglekar's window function

Joglekar's window function is given as:

$$f(x) = [1 - (2x - 1)^{2p}] \tag{1.12}$$

Here p is a positive integer which controls the change in the flatness of $f(x)$ curve around its peak value i.e. $x = 0.5$ [17].

Figure (1.6) shows Joglekar's window function for different values of p. It shows resemblance with a rectangular window function as we increase the p values and provide a reduction in the non-linear drift effect. The major drawback of Joglekar's window function is the flat situation of the state variable at the boundaries, and due to the zero values at both boundaries, it is difficult to change window function.

Joglekar's window function has solved the non-linear drift problem, but it has not considered the boundary lock condition [13, 14].

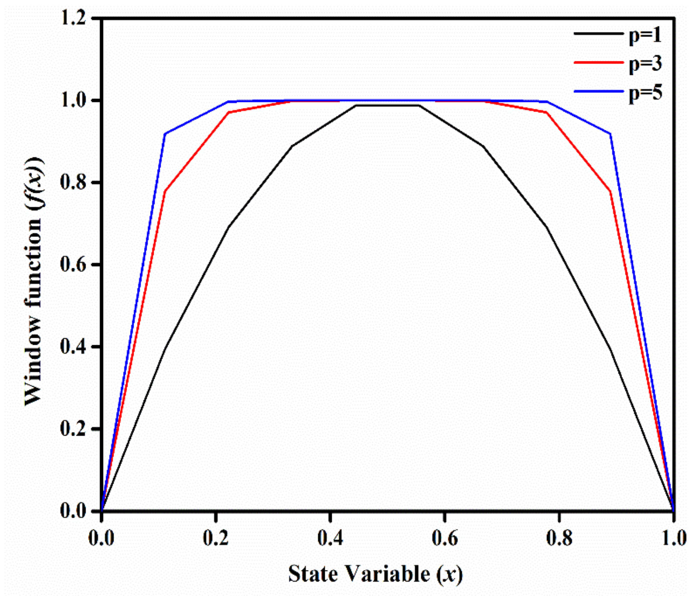

Figure 1.6. Joglekar window function for different p values.

1.2.4. Strukov window function

Strukov window function can be given as

$$f(x) = x - x^2 \tag{1.13}$$

Strukov window function supports the boundary conditions, but some other problem arises at the terminal states [18].

$$\begin{cases} x \to 0 \\ x \to D \end{cases} \to \frac{dx}{dt} = 0 \tag{1.14}$$

Figure (1.7) shows the Strukov window function. This shows that the external field cannot change the state. Another problem is the assumption made by the window function that is memristor remember the amount of charge passing through it as it remembers the state boundary position.

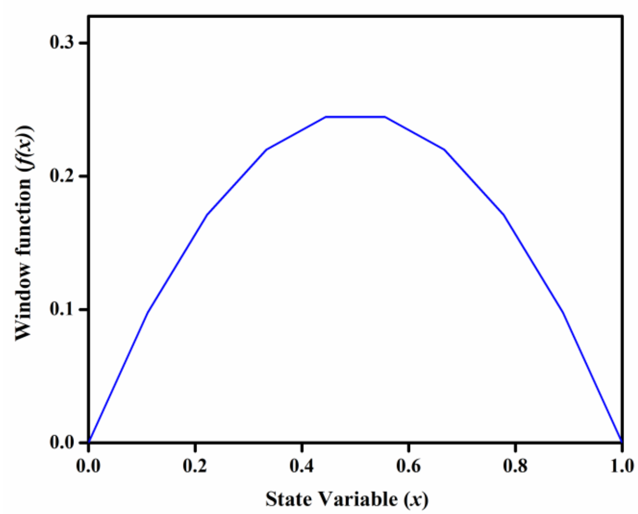

Figure 1.7. Strukov window function.

1.2.5. Exponential model

In the above models, they have not considered a large amount of electric field non-linearity present in the memristor. An exponential model which consider the non-linearity effect has been showed [19]. In this model current-voltage is defined as:

$$I(t) = x^n \beta \sinh\big(\alpha V_i(t)\big) + \chi(e^{(\Upsilon V_i(t))} - 1) \quad (1.15)$$

Where α,β, Υ and χ are experimental fitting parameters.

Influence of state variable on the current is determined by the parameter n [12, 19]. According to Equation (1.15), at ON state, asymmetrical switching behavior is shown by the first part of the equation (1.15) i.e. (sinh part). Whereas at the OFF state, the second part of the Eq. (15) has the major part of the current, which has similar behavior as ideal PN junction [12, 14].

In this model, the rate of change of state variable can be given as:

$$\frac{dx}{dt} = a * V^m * f(x) \quad (1.16)$$

Where m and a are fitting parameters and $f(x)$ represents any window function [14].

1.3 Motivation

Most of the experimental data reported in the literature for various material systems such as WO_3 [20], Y_2O_3 [21], ZnO [22] etc. shows asymmetric behavior in the pinched hysteresis loop in the current-voltage (I-V) characteristics. However, till date, to the best knowledge, a detailed analytical model is unavailable, which could be matched with such experimental hysteresis loop and to analyze the system performance. The developed analytical model, as depicted here, removes this limitation and shows good correlation with experimental data.

1.4 Contributions of the thesis

Here, a new logarithmic window function is proposed to study and analyze the performance of a memristive system. The proposed model is validated with the experimental report on Y_2O_3-based memristive system [21], and window function fulfils all the necessary conditions reported by Prodromakis *et al.* [16]. The proposed window function leads to better non-linear behavior at the device boundaries. Moreover, to eliminate some inconsistencies present in the above models, certain modifications are made in the current-voltage relationship to achieve a better correlation with the experimental data and provide better synaptic behavior analysis.

1.5 Flow chart of analytical modeling

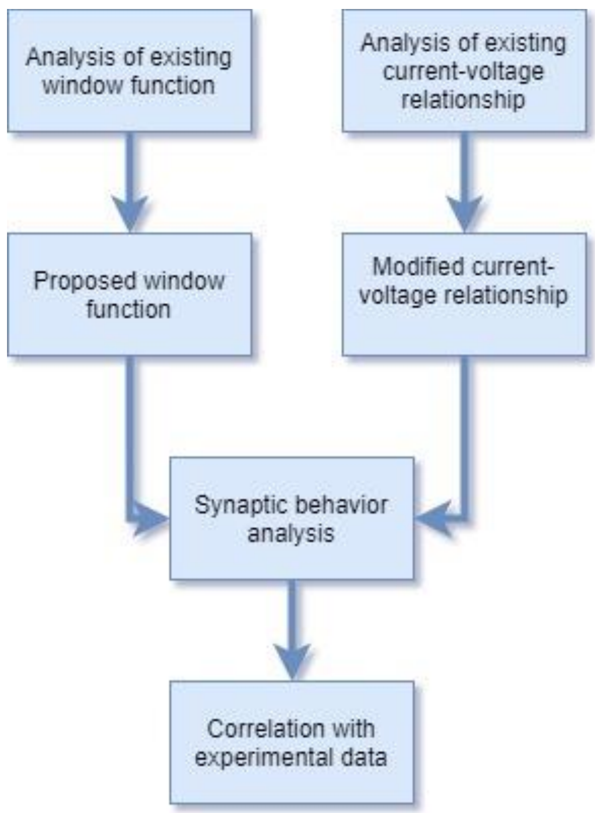

1.6 Organization of the report

This chapter has introduced the background, motivation of the thesis and related work done by researchers in past. The remaining contents are organized as follows:

- Chapter 2: This chapter provides the details about the limitation in the existing window functions and talks about advantage of proposed window function over existing window functions. Section 2.1, Limitation in the existing window functions. Section 2.2, Condition for effective window function. 2.3, Proposed window function. Section 2.4, Correlation with experimental data.

- Chapter 3: This chapter includes the detailed description of modifications in the current-voltage equation, its effect on the V-I characteristics and talks about the advantages of modified current-voltage equation over existing model to achieve better resemblance with the experimental data. Section 2.1, Existing current-voltage equation. Section 2.2, Modified current-voltage equation. Section 2.3, Correlation with experimental data.
- Chapter 4: In this chapter we will discuss the implementing of memristor in a neural computing architectures and talk about the potentiation (P) and depression (D) process of the device while studying the synaptic behavior. Section 2.1, Memristor as Synapses. Section 2.2, Potentiation (P) and depression (D) process. Section 2.3, Applied signal properties and correlation with experimental data.
- Chapter 5: Results and Discussion.
- Chapter 6: Conclusions and Future Work.

Chapter 2

Analysis of window function

This chapter provides the details about the limitations in the existing window functions and talks about advantage of proposed window function over existing window functions and shows the correlation with experimental results.

2.1 Limitation in the existing window functions.

The linear model of the memristor faces major issues such as:

- Boundary issue
- Absence of nonlinearity.

In case of the linear drift model window functions were used to introduce the non-linearity in the ion drift to overcome the boundary issue, this model is known as non-linear drift model. But it was seen from simulation results of these window functions that the amount of non-linearity resulting from these windows is less than that is depicted by practically fabricated devices.

2.2 Condition for effective window function

An effective window function should satisfy the subsequent conditions for modelling of nonlinearity [16]:

- The boundary situation should be taken into consideration at the bottom and top electrodes.
- The window function should provide non-linear drift across the whole active area of the memristor.
- The window function should provide linkage between the linear and non-linear drift models.
- The window function should lie in the interval of $fmax(x)$ i.e. $0 \leq fmax(x) \leq 1$.
- The window function should include some of the control parameters to line the model.

To provide the above criteria's many window function are proposed.

2.3 Proposed window function

Till now all the window functions present in the literature have various problems, so there is a requirement to develop a window function which satisfy certain condition:

- It should provide nonlinearity i.e., with a logarithmic or parabolic kind of relation.
- There should be limit on memristance and state variable that they cannot grow beyond the device physical limit.
- It should be function of state variable and input signal.

- Step function should be avoided so that it cannot show discontinuity at boundaries.

To overcome the problem present in existing windows functions i.e. boundary lock, scalability, and nonlinear effects an accurate window function is proposed show in Figure (2.1)

The proposed window function is given by equation (2.1)

$$f(x) = \log\frac{1}{(x^2-x+1)^p} \tag{2.1}$$

where p is the Parameter for bounding window function between 0 and 1

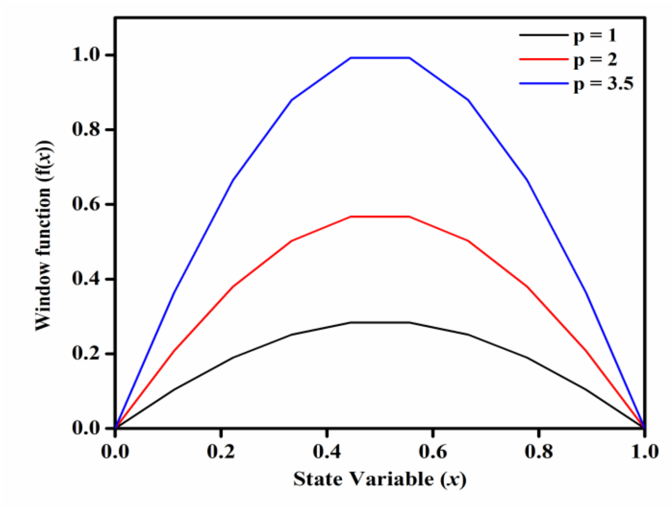

Figure 2.1. Proposed logarithmic window function.

2.4 Correlation with experimental results

Here we have used the proposed window function along with the existing non-linear drift model [19] to analyze the correlation with the experimental results [21].

The current-voltage relationship for existing non-linear model is given by equation (2.2)

$$i(t) = x^n\beta \sinh\big(\alpha V(t)\big) + \chi(e^{(\Upsilon V(t))} - 1) \tag{2.2}$$

The first term of equation (2.2) describes the asymmetric behavior of the device. The second term of equation (2.2) represents the ideal diode equation. Where x is the state variable and χ, α, Υ and β are experimental fitting parameters.

The change in state variable is defined by equation (2.3) for memristive devices.

$$\frac{dx}{dt} = a * V^m * f(x) \tag{2.3}$$

Here $f(x)$ is the window function and describes by equation (2.1) and a , m are fitting parameters.

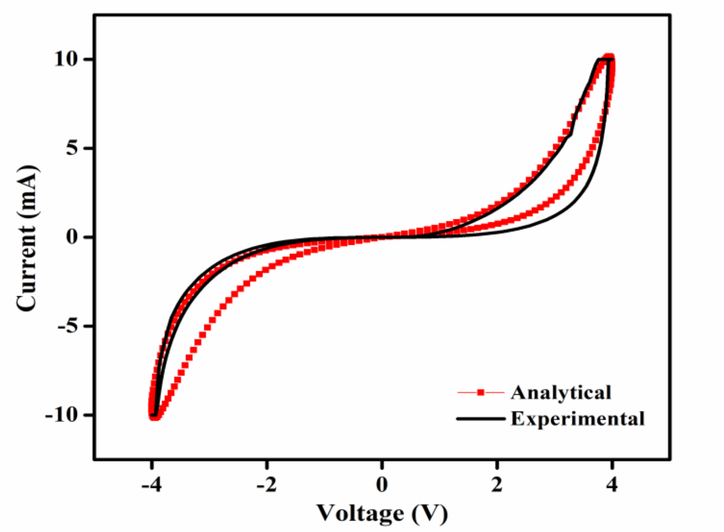

Figure.2.2: I-V characteristic

Here we are using triangular wave with a peak to peak amplitude of 5V to provide similar conditions used in experimental data to provide specific characteristics. Therefore, using above relation, we can see the pinched hysteresis loop characteristics which are the primary footprint of memristor [1] and also provide good resemblance with the experimental data but only for positive values of voltage [21]. For negative values, we see symmetric behavior.

As experimental I-V characteristics are asymmetric, our proposed models are not sufficient for overall analysis. So, to overcome the problems, we have also modified the I-V relationship.

Chapter 3

Analysis of current-voltage relationship

This chapter includes the detailed description of modifications in the current-voltage equation, its effect on the V-I characteristics and talks about the advantages of modified current-voltage equation over existing model to achieve better resemblance with the experimental data.

3.1 Existing current-voltage equation

The existing [19] non-linear model, as reported in the literature, is described by (3.1)

$$i(t) = x^{n}\beta \sinh\big(\alpha V(t)\big) + \chi(e^{(\Upsilon V(t))} - 1) \tag{3.1}$$

Here, x shows the state variable of the memristor, n is the free parameter to control the non-linear dependence of the drift velocity on the applied voltage, α and β are the fitting constants used to characterize the ON state, χ and Υ are the net electronic barrier in the OFF state of the device. The first term leads to flux-controlled memristor with symmetric behavior of the device for both positive and negative polarities of the applied voltage. Thus, it is necessary to make certain improvements in the model to achieve better resemblance with the experimental data, having asymmetric characteristics in positive and negative cycles of applied voltage.

3.2 Modified current-voltage equation

The current-voltage relationship for our model is given by equation (3.2).

$$i(t) = \begin{cases} x^{n_1}\beta_1(e^{\alpha_1(sinhV_i(t))} - 1) + \chi(e^{(\Upsilon V_i(t))} - 1), & V_i(t) \geq 0 \\ x^{n_2}\beta_1(e^{\alpha_2(sinhV_i(t))} - 1) + \chi(e^{(\Upsilon V_i(t))} - 1), & V_i(t) < 0 \end{cases} \tag{3.2}$$

The first term describes the asymmetric behavior of the device for opposite voltage polarities which is neglected by the previous model and thus introduces parameters α_1 and α_2. These parameters α_1 and α_2 are the degrees of influence of the state variable on current for positive and negative voltage polarities, respectively. The second term of equation (3.2) represents an ideal diode equation which plays a significant role when the state variable approaches zero i.e., the device is near the OFF state. In this equation, some fitting parameters such as β_1,β_2, α_1 and α_2 are used to fit the output characteristics of the memristor device. n_1 and n_2 are the conductivity control parameters of the device for both positive and negative applied voltages, respectively. The conductivity of the device is determined by the migration of oxygen vacancies towards the opposite side. Thus, the current starts flowing as a result of the conducting path formed inside the switching material. Here, V_i is the applied triangular waveform as an input voltage.

Equation (3.3) represents the rate of change of state variable with time. The new logarithmic window function $f(x)$, as depicted in Figure (3.1), ensures that the state variable is bounded between 0 and 1 and it is given by (3.4).

$$\frac{dx}{dt} = a * V^m * f(x) \tag{3.3}$$

$$f(x) = \log \frac{1}{(x^2-x+1)^p} \tag{3.4}$$

Where a and m are the parameters to determine the dependence of the state variable on voltage input and m is always an odd integer to ensure that the opposite polarity of the applied voltage leads to opposite change in the rate of change of state variable.

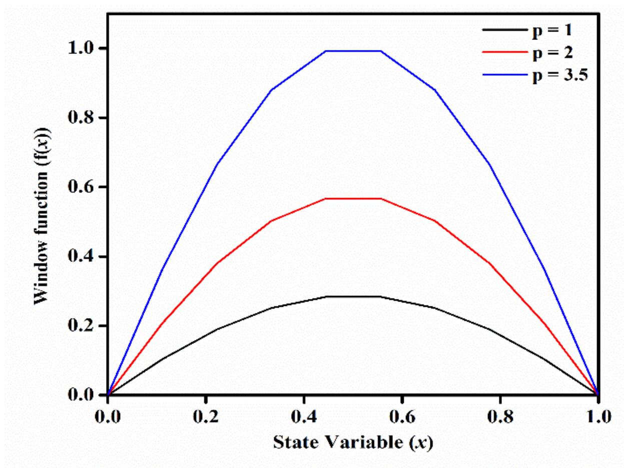

Figure 3.1. Proposed logarithmic window function.

3.3 Correlation with experimental data

Here we have used the same electrical requirements as stated in experimental data for the analysis of the characteristics of Y_2O_3-based memristive system [21]. To study the I-V characteristics of the yttrium oxide based memristive system, a triangular voltage waveform is applied on the device with a peak-to-peak voltage of -5 to 5V with a compliance current of 10 mA. Figure (3.2) and Figure (3.3) shows the similarity between analytical and experimental current behavior [21].

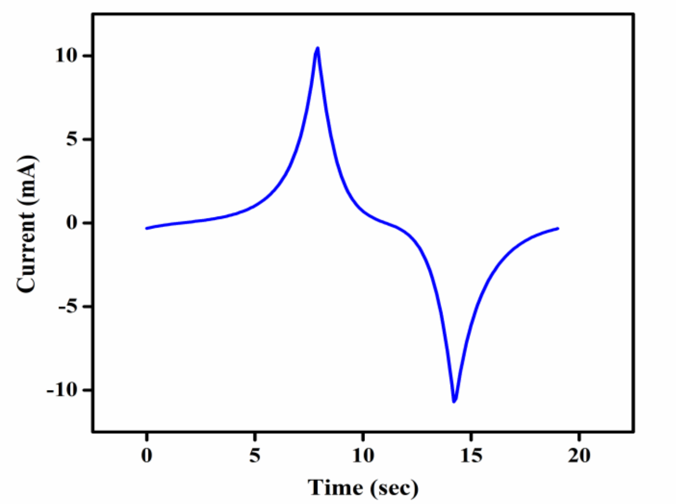

Figure 3.2. Analytical Current Behavior.

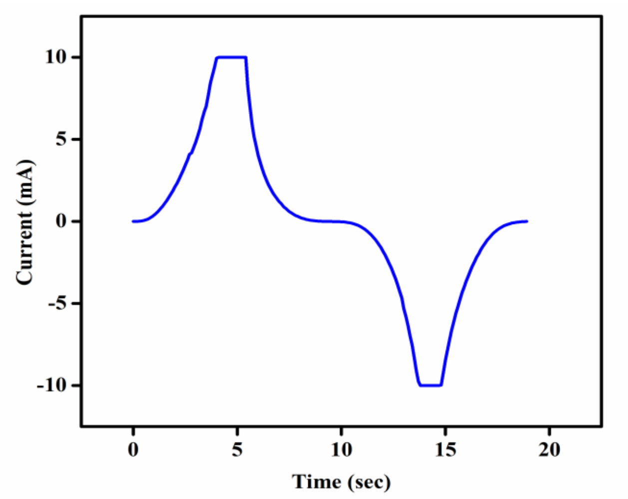

Figure 3.3. Experimental Current Behavior.

Figure (3.4) presents the analytical fitting of the *I-V* characteristics, which shows a better resemblance with the experimental reported data [21] of the device and provides asymmetric behavior.

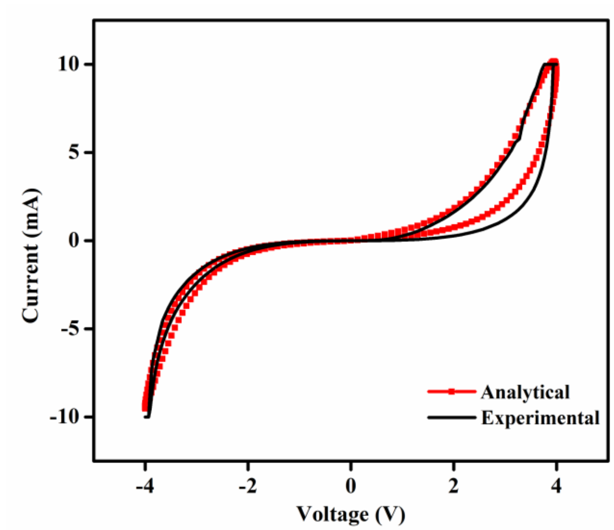

Figure 3.4. I-V characteristics.

Chapter 4

Study of the synaptic behavior

In this chapter we will discuss the implementing of memristor in a neural computing architectures and talk about the potentiation (P) and depression (D) process of the device while studying the synaptic behavior.

4.1 Memristor as Synapses

Neurons and synapses together form neural networks (Figure 4.1), which are the building blocks that provide humans with the ability to learn, think, and remember [23]. A human brain contains ~1010 neurons, each connecting to ~104 other ones. At each connection, there is a junction called a synapse, so there are ~1014 synapses in a human brain. A key quality of the brain's computing power is that the synapses are "plastic". That is, the synaptic weight associated with each synapse can be modulated by signals (action potentials) generated from the two neurons joining the synapse, and the new synaptic weight can be retained. The synaptic weight, in turn, determines the transmission between these the neurons. Thus, *synaptic plasticity,* along with the very large *synaptic connectivity* empowers the efficient brain-based computing paradigm. Merely speaking, synaptic plasticity ensures learning ability while connectivity provides parallel processing capacity.

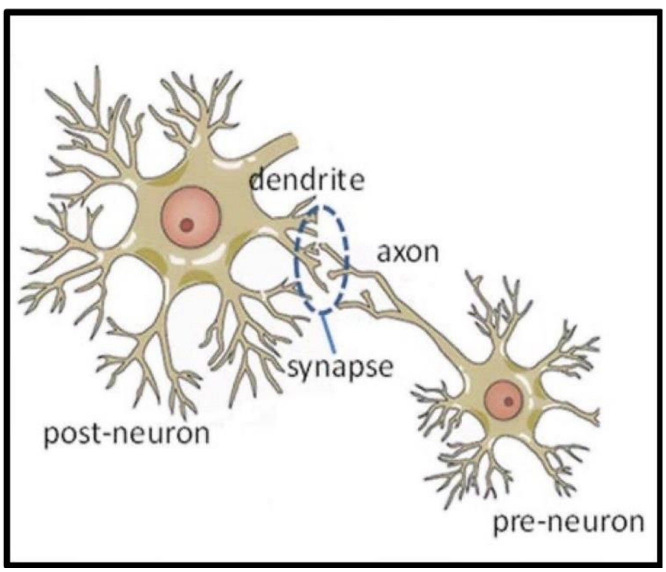

Figure 4.1 Illustrations of a neuron pair connected by a synapse [23]

4.2 Potentiation (P) and depression (D) process

The device used as an artificial synapse must provide conduction from LCS to HCS or from HCS to LCS on the electrical excitation [24].

To replicate the working of biological synapses, major research works are done on memristive devices, which are analyzed over a previous couple of years for non-volatile memory applications, due to their high scalability and low energy consumption.

These devices, when provided with electrical excitation, shows a change in their conductance from SET to RESET states and vice-versa.

The same concept can be used for the neuromorphic applications to provide the potentiation (increasing conductance) and depression (decreasing conductance) behavior in an artificial synapse. For this, several programming based models have been proposed which are based on the application of voltage pulses with varying amplitudes.

4.3 Applied signal properties and correlation with experimental data

During the potentiation process, 50 consecutive positive rectangular pulses followed by 50 rectangular negative pulses with amplitude of 4V and pulse-width of 5µs is applied on the device. Under positive pulses, the synaptic weight, i.e. the device conductance increases continuously with the number of stimulating positive pulses and decreases subsequently for the negative pulses.

This behavior is similar to the learning behavior of the human brain, where the synaptic strength of the neuromorphic system changes according to the number of stimuli received during the learning process. This behavior is similar to the learning behavior of the human brain, where the synaptic strength of the neuromorphic system changes according to the number of stimuli received during the learning process.

Thus, the continuous strengthening and weakening in synaptic weight defined by the potentiation and the depression processes where the former relates to the learning function of the brain and the latter are analogous to the forgetting process of the human memory.

Chapter 5

Results and Discussion

In this chapter, we have discussed results of proposed method. Proposed window function and its correlation with the experimental result. Modified current equation, its behavior and correlation of I-V characteristics with the reported experimental data. Conductance and actual power analysis. Synaptic behavior of memristive device and its correlation with the experimental data using figures and tables.

5.1 Propose window function

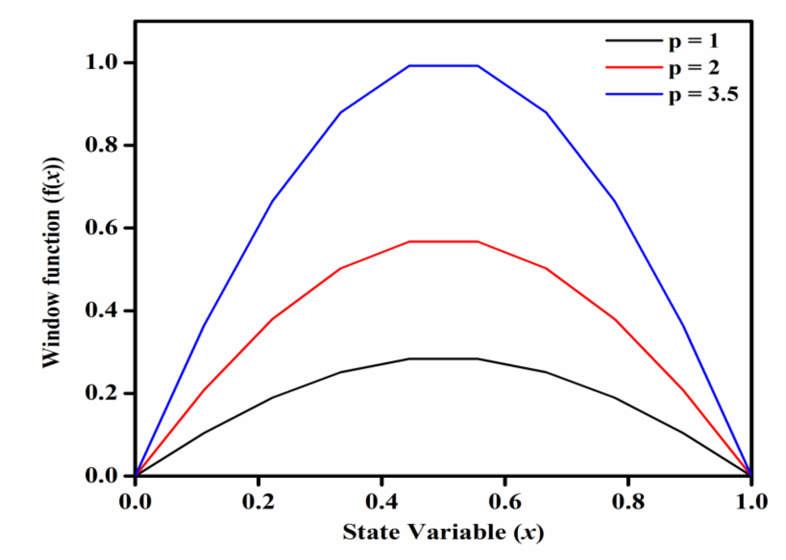

Figure 5.1: Window Function

The proposed window function shown in Figure (5.1) has a maximum value at ($x = .5$) and zeroes at the boundaries ($x = 0$ and $x = 1$).

The drift ion model given by HP laboratories [2] doesn't provide linear property at the boundaries and shows boundary lock problem, i.e. the drift velocity of oxygen vacancy becomes zero at ($x = 0$ and $x = 1$). Since oxygen vacancy becomes zero, the state variable is locked at the boundary, i.e. (0 and D).

The proposed window function shown in Figure (5.1) removes issues present in Chau's postulates [1], provide better switching and proportional relationship between charge and state variable, which in terms provides better non-linear memristor behavior.

5.1.1 Pinched hysteresis current-voltage characteristics of memristive device:

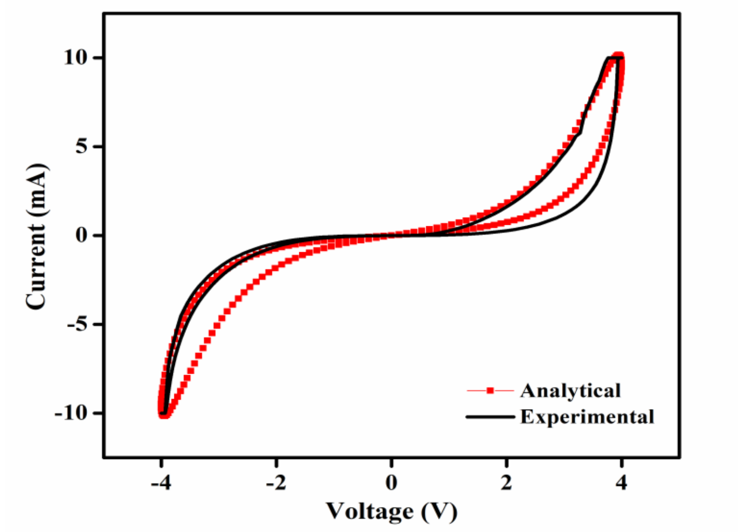

Figure.5.2: I-V characteristic

To analyse the various characteristics of memristor, a triangular waveform with a peak-to-peak amplitude of 5V is applied. Figure (5.2), is the I-V characteristics of memristor, which shows the pinched hysteresis switching behavior and provide good R square score ~92% with the experimental result but failed to show asymmetric behavior present in the I-V characteristics.

5.1.2 Conductance:

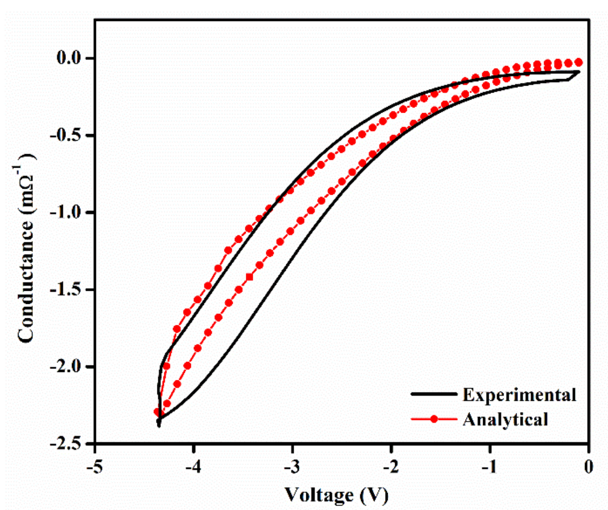

Figure.5.3: Conductance vs. Voltage

The variation of conductance with the applied negative voltage (0 to -5) is shown in Figure (5.3). Here negative behavior of conductance with the applied voltage (0 to -5) shows the opposite flow of current in the memristive device and provides good R square score of ~94.2% with experimental data [21].

Practically conductance is a positive quantity.

5.1.3 Synaptic behavior of memristive devices:

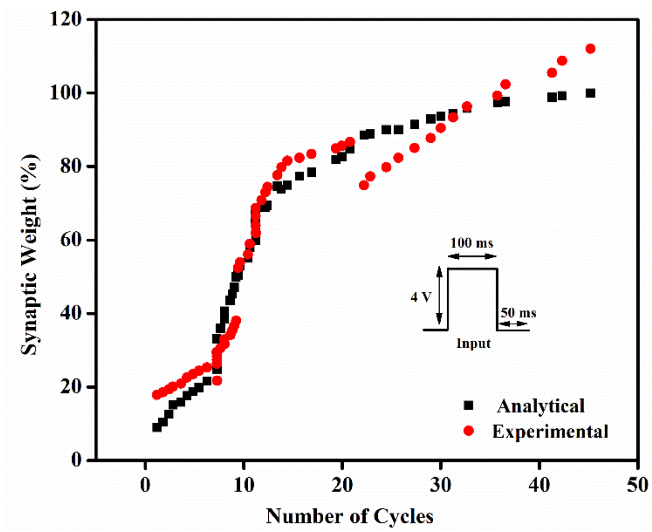

Figure.5.4: Synaptic Weight vs. Number of Cycles

In the case of synaptic weight, we have applied a rectangular voltage pulse of amplitude 4V and duty cycle 66 percentage. Figure (5.4) presents the analytical fitting of the synaptic weight characteristics, which shows a better resemblance with the reported experimental data of the device.

But from the above Figure (5.4) it can be seen that the accuracy for potentiation (increasing conductance) process is ~82 percentage. Also, it is not possible to achieve depression (decreasing conductance) process in our model.

5.2 Modified current-voltage relationship

To overcome the issue present in the proposed window function model, we have modified the current-voltage relationship in non-linear drift model, which provides good resemblance with the experimental data.

5.2.1 Current-voltage characteristics of memristive device:

To analyse the switching characteristics of memristor, a triangular waveform with a peak-to-peak amplitude of 5V is applied. Figure (5.5), is the I-V characteristics of memristor, which shows the pinched hysteresis switching behavior and provide good R square score ~98% with the experimental result.

The modified current equation also overcomes the problem of asymmetric behavior present in the I-V characteristics shown in Figure (5.2).

According to Chua, any device such as RRAM to belong in the memristive device category must show pinched hysteresis loop characteristics [1].

As the pinched hysteresis loop is the primary footprint of the memristive device we can make some observations such as:

- The I-V characteristics of memristor is always limited to the 1st and 3rd quadrant which indicates device is passive.
- The pinched hysteresis loop is bounded between a maximum and minimum value of resistance i.e. R_{ON} and R_{OFF}.
- The I-V characteristics of memristor always crosses the origin which means that once the input signal is removed from the device the output is always forced to zero.
- As the frequency of the applied signal increases the pinched hysteresis loop shows the singled valued function and behaves as a linear resistor.

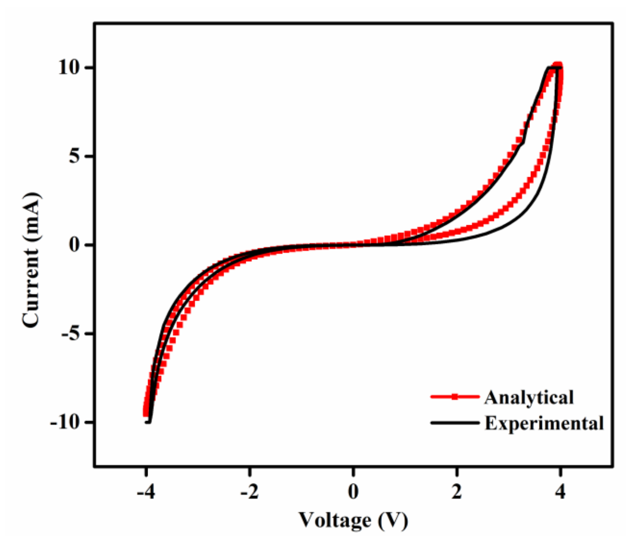

Figure.5.5: I-V characteristic

To provide better resemblance with the experimental data, various fitting parameters present in the current-voltage relationship has been varied, and most appropriate values have been taken in this thesis which can be seen in the Table (1).

Parameters	Numerical Values	Physical interpretation
n	5	Hysteresis loop broadness control parameters
β	0.009	Experimental fitting parameters
α	1	Experimental fitting parameters
χ	0.0004	Magnitude of ideal diode behavior
ϒ	1	Diode parameters like thermal voltage and ideality factor
m	Odd integer	Control the effect of input on the state variable
a	0.001	Control the effect of the window function
p	2	Parameter for bounding window function between 0 and 1

Table 1: Numerical values and physical interpretation of parameters

5.2.2 Actual power:

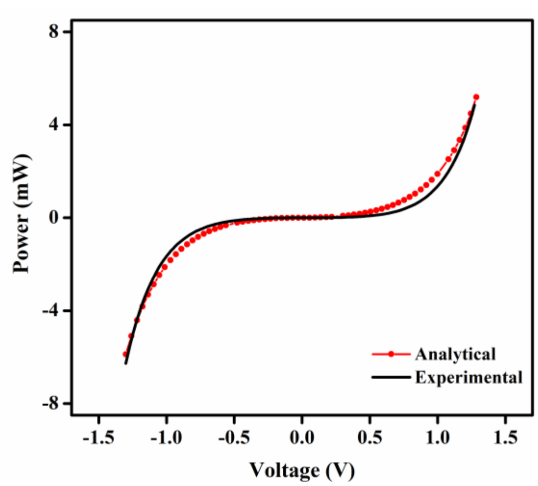

Figure.5.6: Power vs. Voltage

Figure (5.6) shows the actual power characteristics of device which is showing good R square score ~98% with the experimental data.

The power consumption in memristor mainly depends on the following factors:

- applied voltage
- current generated
- pinched hysteresis loop width

Any variation in the above factors affects the power consumption of a device

The negative part of the curve provides the detail of power consumption for the negative polarity of the applied voltage

5.2.2 Synaptic behavior of memristive devices:

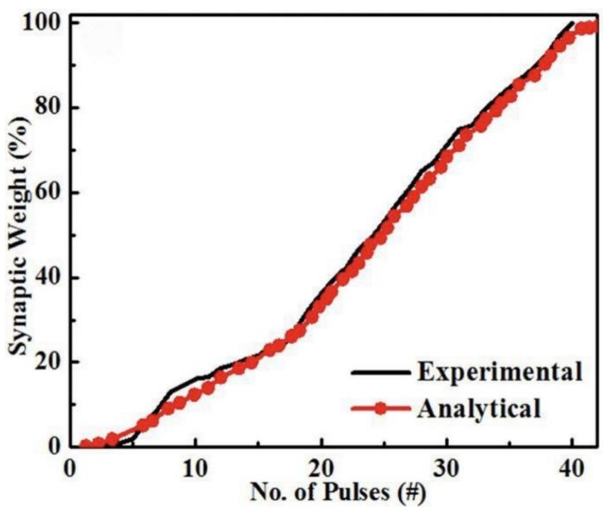

Figure 5.7. Potentiating characteristics of device

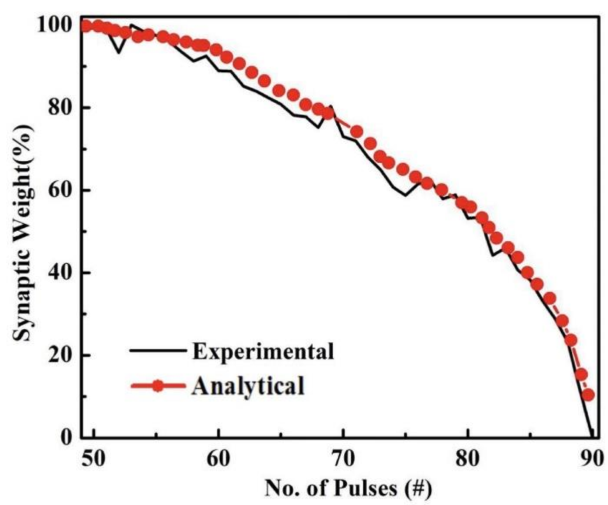

Figure 5.8. Depressing characteristics of device

On the application of positive and negative pulses, the value of conductance increases or decreases and also the depression and potentiation in the biological synapse.

On the application of a train of 50 positive rectangular pulses with a peak to peak value of 4V and pulse width 100ms, we can see the strengthening in the synaptic weight (potentiation process) while on the application of 40 negative rectangular pulses with the peak to peak value of -4V and pulse width 100ms, we can see the gradual weakening of synaptic weight (depression process).

The potentiating and depressing characteristics of the device is shown in Figure (5.7) and Figure (5.8), which are very useful for device synaptic weight modulating.

From Figure (5.7) and Figure (5.8), it can be seen that the proposed method in the thesis is providing a good R square score ~98.2% with the experimental data.

The percentage R-square score of various graphs can be seen in Table (2).

Name of Parameter	Accuracy with experimental data	Error with experimental data
Current-Voltage(I-V) Characteristics	~98%	~2%
Conductance	~94.2%	~5.8%
Actual power	~97.36%	~2.24%
Synaptic behavior	~98.12%	~1.78%

Table 2: R squared (R2) % score with Experimental Data

Chapter 6

Conclusions and Future Work

6.1 Conclusions

Here, Y_2O_3-based memristive switching characteristics have been examined using an analytical model with a new logarithmic window function and a modified I-V relationship for neuromorphic applications. The previous model had several discrepancies with the experimental data, such as the absence of a parameter to account for asymmetric nature of loop in the positive and negative voltage cycles. Our model successfully removes this problem by defining suitable parameters. The model is found to provide good resemblance with the learning and forgetting processes of the human brain through the potentiating and the depressing process, respectively. For the future evolution of the devices for realizing the hardware implementation of neural systems, these properties of memristors are convenient and useful.

6.2 Future Work

This model has removed several discrepancies which were present in the other models and provided proper parameters for the analyses of experimental results which help in the study of synaptic behavior of a Y_2O_3 based memristive system. Memristors can be found useful in various neuromorphic hardware and machine learning-based systems. Among which memristor-based image processing systems are most prominent.

REFERENCES

[1] Chua LO. Memristor-the missing circuit element. IEEE Transaction Circuit Theory. 1971; 18(5):507-519. DOI: 10.1109/TCT.1971.1083337

[2] Strukov DB, Snider GS, Stewart DR, Williams RS. The missing memristor found. Nature Letter. 2008; 453:80-83. DOI: 10.1038/nature06932

[3] Dongale TD. Development of High Performance Memristor for Resistive Random Access Memory Application [Thesis]. Kolhapur Maharashtra, India: Shivaji University; 2015

[4] Georgiou PS. A Mathematical Framework for the Analysis and Modelling of Memristor Nanodevices [Thesis]. London: Chemistry of Imperial College London; 2013

[5] Kavehei O. Memristive Devices and Circuits for Computing, Memory, and Neuromorphic Applications [Thesis]. Australia: The University of Adelaide; 2011

[6] Adhikari S, Sah M, Kim H, Chua L. Three fingerprints of memristor. IEEE Transactions on Circuits and Systems I: Regular Papers. 2013;60(11):3008-3021. DOI: 10.1109/TCSI.2013.
2256171

[7] Chua LO. Resistance switching memories are memristors. Applied Physics A. 2011;102:765-783. DOI: 10.1007/s00339-011-6264-9

[8] Gul F, Efeoglu H. ZnO and ZnO_{1-x} based thin film memristors: The effects of oxygen deficiency and thickness in resistive switching behavior. Ceramics International.2017;43(14):10770-10775. DOI: 10.1016/j.ceramint.2017.05.090

[9] Gul FE, Efeoglu H. Bipolar resistive switching and conduction mechanism of an Al/ZnO/Al based memristor. Superlattices and Microstructures. 2017;101:172-179. DOI: 10.1016/j. spmi.2016.11.043

[10] Mehonic A, Cueff S, Wojdak M, Hudziak S, Jambois O, Labbé C, Garrido B, Rizk R,Kenyon AJ. Resistive switching in silicon suboxide films. Journal of Applied Physics.2012;111(7):074507. DOI: 10.1063/1.3701581

[11] Wang Q, Sun HJ, Zhang JJ, Xu XH, And Miao XS. Electrode materials for Ge2Sb2Te5-based memristors. Journal of Electronic Materials. 2012;41(12):3417-3422. DOI: 10.1007/s11664-012-2256-6

[12] Elgabra H, Farhat IAH, Al Hosani AS, Homouz D, Mohammad B. Mathematical modeling of a memristor device. In: 2012 International Conference On Innovations in Information Technology (IIT); 18-20 mar 2012; Abu Dhabi, United Arab Emirates: IEEE; 2012. pp.156-161

[13] Zha J, Huang H, Liu Y. A novel window function for memristor model with application in programming analog circuits. IEEE Transactions On Circuits and Systems—II: Express Briefs. 2016;63(5):423-427. DOI:0.1109/TCSII.2015.2505959

[14] Radwan AG, Fouda ME. On the Mathematical Modeling of Memristor, Memcapacitor, and Meminductor. Springer; 2015. p. 244. DOI: 10.1007/978-3-319-17491-4

[15] McDonald NR, Pino RE, Rozwood PJ, Bryant TW. Analysis of dynamic linear and nonlinear memristor device models for emerging neuromorphic computing hardware design.In: 2010 IEEE International Joint Conference on Neural Networks (IJCNN); 18-23 July 2010; Barcelona, Spain: IEEE; 2010. pp. 1-5

[16] Prodromakis T, Peh BP, Papavassiliou C, Toumazou C. A versatile memristor model with non-linear dopant kinetics. IEEE Transactions on Electron Devices. 2011;58(9):3099-3105.DOI: 10.1109/TED.2011.2158004

[17] Joglekar YN, Wolf SJ. The elusive memristor: Properties of basic electrical circuits. European Journal of Physics. 2009;30(4):661-675. DOI: 10.1088/0143-0807/30/4/001

[18] D. B. Strukov, G. S. Snider, D. R. Stewart, and R. S. Williams, “The missing memristor found,” Nature, vol.453, no. 7191, pp. 80–83, 2008.

[19] Yang JJ, Pickett MD, Li X, Ohlberg DAA, Stewart DR, Williams RS. Memristive switching mechanism for metal/oxide/metal nanodevices. Nature Nanotechnology.2008;3(7):429-433.DOI: 10.1038/nnano.2008.160

[20] T. Chang, S. H. Jo, K. H. Kim, P. Sheridan, S. Gaba, W. Lu, “Synaptic behaviors and modeling of a metal oxide memristive device,” Applied Physics A, vol. 102, pp.857–863, 2011.

[21] M. Das, A. Kumar, R. Singh, M. T. Htay and S.Mukherjee, “Realization of synaptic learning and memory functions in Y_2O3 based memristive device fabricated by dual ion beam sputtering,” Nanotechnology, vol. 29, no.055203, pp. 1-9, 2018.

[22] A. Kumar, M. Das, V. Garg, B. S. Sengar, M. T. Htay,S. Kumar, A. Kranti, and S. Mukherjee, “Forming-free high-endurance Al/ZnO/Al memristor fabricated by dual ion beam sputtering,” Applied Physics Letters**,** vol. 110, no. 253509, pp. 1-5, 2017

[23] J. W. Rudy, *The Neurobiology of Learning and Memory*; Sinauer Associates, Inc. Publishers, 2008

[24] E.Covi, Sb Brivio, M. Fanciulli, S. Spiga,”Synaptic potentiation and depression in Al: HfO_2,” Microelectronic engineering; 147; 41-44; 2015. DOI: 10.1016/j.mee.2015.04.052